POLISH POLAR RESEARCH
vol. 40, no. 4, pp. 311–338, 2019 doi: 10.24425/ppr.2019.130901

Importance of snow as component of surface mass balance of Arctic glacier (Hansbreen, southern Spitsbergen)

Aleksander USZCZYK[1*], Mariusz GRABIEC[1], Michał LASKA[1], Michael KUHN[2] and Dariusz IGNATIUK[1]

[1] *University of Silesia in Katowice, Faculty of Natural Sciences, Będzińska 60, Sosnowiec, Poland*

[2] *Institute of Atmospheric and Cryospheric Sciences, University of Innsbruck, Innrain 52, A-6020 Innsbruck, Austria*

[*] *corresponding author <aleksanderuszczyk@gmail.com>*

Abstract: Snowmelt is a very important component of freshwater resources in the polar environment. Seasonal fluctuations in the water supply to glacial drainage systems influence glacier dynamics and indirectly affect water circulation and stratification in fjords. Here, we present spatial distribution of the meltwater production from the snow cover on Hansbreen in southern Spitsbergen. We estimated the volume of freshwater coming from snow deposited over this glacier. As a case study, we used 2014 being one of the warmest season in the 21st century. The depth of snow cover was measured using a high frequency Ground Penetrating Radar close to the maximum stage of accumulation. Simultaneously, a series of studies were conducted to analyse the structure of the snowpack and its physical properties in three snow pits in different glacier elevation zones. These data were combined to construct a snow density model for the entire glacier, which together with snow depth distribution represents essential parameters to estimate glacier winter mass balance. A temperature index model was used to calculate snow ablation, applying an average temperature lapse rate and surface elevation changes. Applying variable with altitude degree day factor, we estimated an average daily rate of ablation between 0.023 m d^{-1} $°C^{-1}$ (for the ablation zone) and 0.027 m d^{-1} $°C^{-1}$ (in accumulation zone). This melting rate was further validated by direct ablation data at reference sites on the glacier. An average daily water production by snowmelt in 2014 ablation season was 0.0065 m w.e. (water equivalent) and $41.52 \cdot 10^6$ m^3 of freshwater in total. This ablation concerned 85.5% of the total water accumulated during winter in snow cover. Extreme daily melting exceeded 0.020 m w.e. in June and September 2014 with a maximum on 6th July 2014 (0.027 m w.e.). The snow cover has completely disappeared at the end of ablation season on 75.8% of the surface of Hansbreen.

Key words: Arctic, Svalbard, snowpack, snow accumulation and ablation, snow water equivalent, temperature index model.

Introduction

The climate change observed during the last few decades manifests itself, especially in the Arctic, by remarkable warming and precipitation rise (Miller *et al*. 2010; Koenigk *et al*. 2015; Łupikasza *et al*. 2019) which both may significantly change the properties of the snow cover (Christensen *et al*. 2007; Räisänen 2008; Sturm *et al*. 2010) that is a vital component of Arctic environment. The snow cover substantially affects the functioning of glacial systems, and particularly their mass balance (Fujita 2008; Benn and Evans 2010). As a consequence of environmental changes, the snow depth and snow water equivalent (SWE) as well as the internal structure of the snowpack, may vary from year to year and thereby influencing fresh water runoff and its time of release (Hartman *et al*. 1999; Marsh 1999; Bruland *et al*. 2004). The snow as a source of meltwater is a factor influencing the glacier drainage system (Fountain 1996a, 1996b; Decaux *et al*. 2019) and supplies the water that percolates in the firn area and controls internal accumulation and water storage (Fountain 1989; Pfeffer and Humhprey 1998; Jansson *et al*. 2003; Parry *et al*. 2007). As meltwater is one of the main factors determining glacier movement (Willis 1995; Vieli *et al*. 2004; van Pelt *et al*. 2018), knowledge of snow properties, its spatial distribution and mass turnover helps to understand glacier dynamics. Finally, meltwater runoff to the Arctic fjords influences their stratification and water circulation (Cowan 1992; Straneo *et al*. 2011; Mortensen *et al*. 2013; Carroll *et al*. 2015).

Svalbard is one of the most vulnerable areas in the Arctic. The highest recent warming in the European sector of the Arctic at the rate of 2.6°C per century (Nordli *et al*. 2014), and increase of annual precipitation by 2.5% per decade since the beginning of the 20th century (Førland and Hanssen-Bauer 2003) give a unique opportunity to investigate the impact of those processes on the snow cover. Climate change is reflected by the general mass loss of Svalbard glaciers, however the most negative mass balance is reported for southern Spitsbergen (Nuth *et al*. 2010, 2013; Möller *et al*. 2016; Aas *et al*. 2016; Błaszczyk *et al*. 2019b). This suggests that in southern Spitsbergen most water accumulated in the snow during the winter feeds glacier systems in summer and may exert stronger influence on glacial processes than at other Arctic sites. We selected Hansbreen for the current study, a typical Svalbard tidewater glacier located in Hornsund area (southern Spitsbergen) with long and continuous glaciological and meteorological data series, as well as rich snow studies (*e.g*., Migała *et al*. 1988; Winther *et al*. 2003; Grabiec 2005; Grabiec *et al*. 2006, 2011; Laska *et al*. 2016, 2017a, 2017b). Due to the dynamic environmental changes in this area, Hansbreen may serve as an analogue for the analysis of glacial processes driven by meltwater of snow origin on most glaciers all over the Arctic.

Here, we analysed snow accumulation and ablation during the season 2013/2014, to estimate glacier-wide snow balance on Hansbreen and to identify

how much freshwater is produced from the seasonal snow cover during specific ablation periods and is supplied to the glacier surface and its drainage system. The dynamics and intensity of nival processes mentioned above leading finally to the water output, is determined by complex process of the snow cover evolution on the Arctic glaciers. During the accumulation season, the snow cover is formed and modified by meteorological conditions, particularly precipitation, which form depends on air temperature (*e.g.*, Dai 2008; Krasting *et al.* 2013). Snow distribution on the glacier also depends on wind speed and direction, and local topography. The occurrence of local depressions may favour snow accumulation. Melting processes over the snow surface during mid-winter thaw periods significantly influence the variability of snow properties. Meltwater may percolate downwards, refreeze within lower layers, thereby increasing their density. Thus, winter thaws do not necessarily translate into a release of meltwater from snow cover to the glacier. A similar process takes place during rain episodes in winter (Łupikasza *et al.* 2019). During the ablation season, the snow cover can be completely saturated with liquid water (slush), which in some parts of the glacier refreezes creating superimposed ice (Brandt *et al.* 2008; Irvine-Fynn *et al.* 2011; Grabiec 2017).

The aim of this paper is to show the spatial distribution of winter accumulation and summer snow melting, as well as temporal pattern of meltwater release from the snow cover. Detailed snow studies allow to precisely assess the snow contribution to the glacier mass balance. This survey helps also to understand spatial and temporal differences in glacial processes in the Arctic driven by variable rate and intensity of snow cover formation, evolution and decay. The main purpose of the study was to establish the role of the snow cover in the glacier system, paying particular attention to the importance of snowmelt water. The ice melt during the ablation season has not been considered at all.

The Temperature Index Model (TIM) (*e.g.*, Braithwaite 1995; Hock 2003) was chosen for snowmelt assessment due to its simplicity and convenient approach. Glacier surface melt and air temperature are strongly correlated (Braithwaite and Olesen 1989), making the TIM model particularly useful whenever temperature data is available (Ohmura 2001). In this case, temperature and ablation rate data were available at three automatic weather stations on Hansbreen, allowing to estimate snowmelt during an ablation season using TIM. The winter balance was evaluated from shallow Ground Penetrating Radar (GPR) and snow pits analysis providing density data and validating snow depth.

Study area

Hansbreen is a medium sized tidewater glacier (53.8 km^2) located in southern Spitsbergen (Wedel Jarlsberg Land) terminating into Hansbukta, a part of the Hornsund fjord (Ignatiuk *et al*. 2014). It is approximately 16 km long and 2.5 km wide on average. Its boundary is well defined by the surrounding mountains, although it remains linked to Paierlbreen over its north-east passage, Vrangpeisbreen over northern ice-divide and Werenskioldbreen through narrow western passes (Grabiec *et al*. 2012). Four tributary glaciers (Staszelisen, Deileggbreen, Tuvbreen, and Fuglebreen) are located in its western bank (Fig. 1). The glacier front is *ca*. 1.5 km wide, varying among years as a result of glacier dynamics and calving processes (Błaszczyk *et al*. 2009). The glacier's vertical range is *ca*. 550 m and its average ice thickness is *ca*. 171 m, with a maximum at 386 m (Grabiec *et al*. 2012).

The weather conditions over Hornsund area are frequently determined by advection of air masses from the Greenland and Norwegian Sea. Hence, the climate of southern Spitsbergen is considerably warm, humid and more sensitive to variations compared to other Arctic areas (Marsz 2013). The mean multiannual (1978–2014) precipitation sum is *ca*. 439 mm and the average multiannual air temperature is -4.0°C (Marsz 2013) (Table 1). Approximately 30% of the total precipitation in Hornsund occurs in solid form with the largest snowfall contribution between January and April (Łupikasza 2013). Hansbreen mass balance has been widely investigated in previous studies (Szafraniec 2002; Migała *et al*. 2006; Oerlemans *et al*. 2011; Aas *et al*. 2016; Möller *et al*. 2016; Błaszczyk *et al*. 2019b). According to the minimal glacier model of Oerlemans *et al*. (2011) the positive mean surface mass balance of Hansbreen has never recreated its 1900 state. Snow accumulation on Hansbreen is highly variable (Grabiec *et al*. 2006, 2011; Laska *et al*. 2017; Grabiec 2017). The distribution of snow cover on this glacier is strongly modified by snow re-deposition determined by wind speed and direction. According to Styszyńska (2013), prevailing wind directions in Hornsund are NE, E and SE (accounting for over 80% of the wind recorded). The eastern side of Hansbreen is bordered by the Sofiekammen ridge, a natural orographic barrier for advection of air masses, creating a foehn effect during eastern winds (Grabiec *et al*. 2011; Aas *et al*. 2016).

The summer ablation rates are determined mainly by air temperature, direct solar radiation and sunshine duration (Szafraniec 2002). Over the period 1989–2016, mean summer mass balance (B_s) was -1.32 m w.e. with minimum at -1.94 m w.e. in 2016, mean winter mass balance was 0.97 m w.e. with maximum, 1.30 m w.e. in 2006. The average net mass balance (B_n) in period 1989–2006 was -0.35 m w.e. with minimum in 2001 (-1.10 m w.e.) and 2016 (-1.08 m w.e.). However, in year 1994 and 2004–2008, net mass balance was

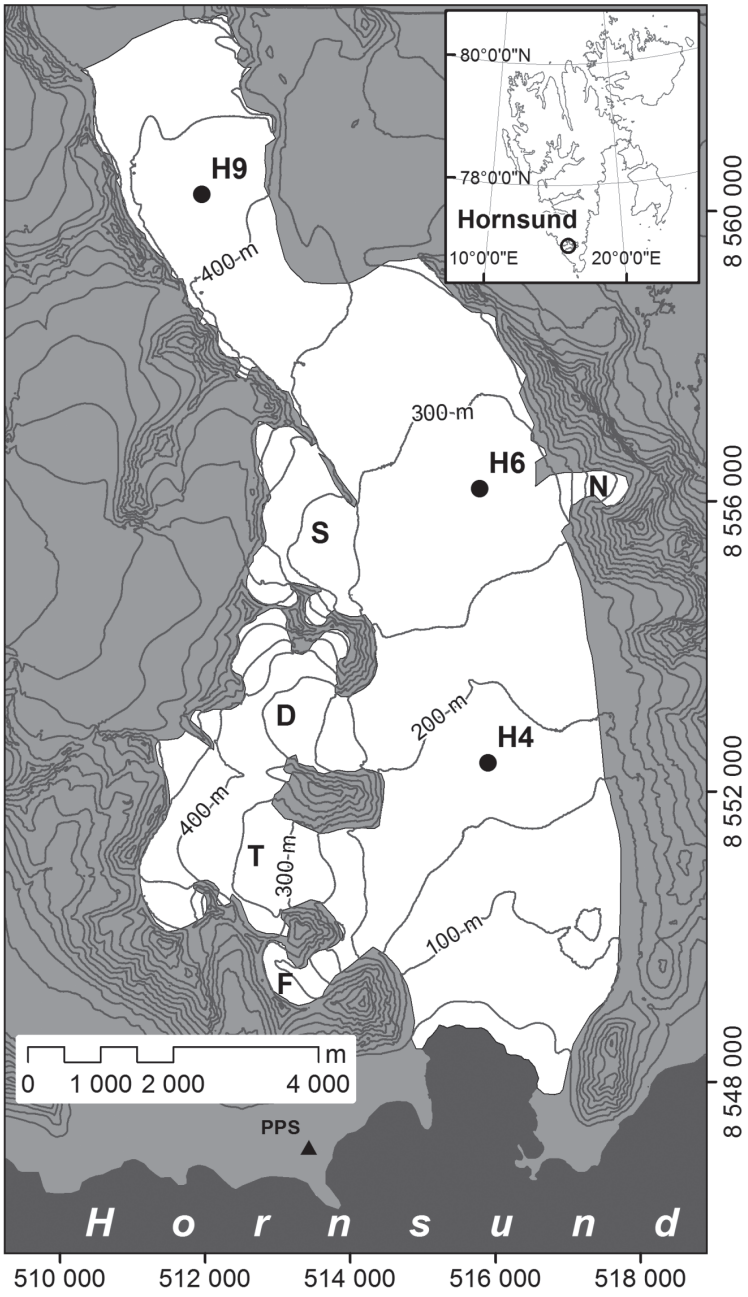

Fig. 1. Study area of Hansbreen. H4, H6, H9 – the automatic weather stations and snow pits sites. Capital letters indicate tributary glaciers: D – Deileggbreen; F – Fuglebreen; N – Nordstebreen; S – Staszelisen; T – Tuvbreen. The UTM zone 33N geodetic system and WGS 1984 datum was used in all maps of this paper.

Table 1

Characteristics of selected meteorological parameters during the accumulation season (09.2013–04.2014), ablation season (05.2014–09.2014) and for the 1978–2014 period at the Polish Polar Station in Hornsund.

	Accumulation season 2013/2014[1,2]	Ablation season 2014[2]	Annual 1978–2014[2]
AIR TEMPERATURE			
Season mean [°C]	-3.5	2.9	-4.0
Minimum	-17.7 (December 2013)	-10.7 (May 2014)	-35.9 (16.01.1981)
Maximum	9.3 (September 2013)	11.9 (August 2014)	13.5 (07.07.2005)
PRECIPITATION			
Season total [mm]	275	188	439
Days with rain	180	98	94
Days with snow	130	32	171
SNOW COVER			
Mean snow depth [cm]	25	13.4	19
Maximum snow depth [cm]	56	47	80
Days with snow cover	203	40	256
Days with snow cover ≥20 cm	26	0	107
WIND			
Mean season wind speed [m s^{-1}]	6.1	5.0	5.6
Days with strong wind (≥10 m s^{-1})	127	180	162

[1] Kępski *et al*. (2013); [2] Łaszyca *et al*. (2014)

close to 0 m w.e. or slightly above (up to 0.15 m w.e. in 2008) (Szafraniec 2002; WGMS 2012, 2015; Błaszczyk *et al*. 2019a, 2019b).

The retreat rate of Hansbreen has been estimated as 40–45 m a^{-1} in period 1989–2000 and 56 m a^{-1} in 2006–2015 (Błaszczyk *et al*. 2013, 2019a). The mean frontal ablation (ice flux and retreat) in 2006–2015 has been calculated as 34.9 Mt a^{-1} (-0.65 m w.e.) (Błaszczyk *et al*. 2019a). The mass losses of this glacier due to surface and frontal ablation far outweigh the gains from winter accumulation, failing reproduce previous glacier states (Szafraniec 2002; Hagen *et al*. 2003) and resulting in a permanently decreasing glacier volume and area.

Therefore, calving and ice flux on Hansbreen and other glaciers in Hornsund area become truly important (Jania *et al*. 1996; Jania and Kaczmarska 1997; Vieli *et al*. 2002; Błaszczyk *et al*. 2009, 2013; Oerlemans *et al*. 2011).

Weather conditions between September 2013 and August 2014

Meteorological observations carried out at the WMO station (no. 010030, 77°00' N, 15°32' E, 10 m a.s.l.) managed by the Polish Polar Station (PPS) provide homogenous data series representative for Hornsund area. For the period analysed here, a snow cover on tundra was present from the beginning of October 2013 to the beginning of June 2014. The melting period started on 16th of May 2014. This year was the second warmest year in the history of the observations at this site, with an annual mean temperature of -1.3°C (Łaszyca *et al*. 2014) and mean temperature in ablation season 2.9°C (Table 1). The air temperature during accumulation season 2013/2014 was significantly warmer than the multiannual average, with the maximum positive deviation in February (9.5°C warmer than the average) (Table 1, Fig. 2).

The sum of precipitation in the accumulation season 2013/2014 and the ablation season 2014 are comparable with more number of days with rain or snow during the accumulation season (Table 1). Heavy snowfalls occurred between March and April 2014 resulting in the most intense snow cover formation (Fig. 3). The duration of the snow cover was overall 20 days shorter than the multiannual mean, however, it reached one of the highest maximum depth (56 cm) since

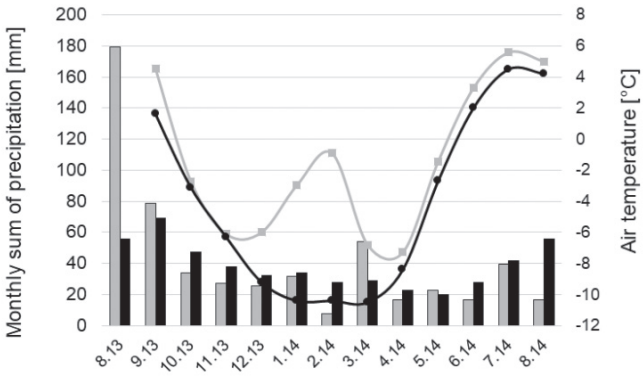

Fig. 2. The mean monthly air temperature (squares) between September 2013 and August 2014 and multiannual (1978–2014) average (dots) at the Polish Polar Station Hornsund (PPS). Monthly sum of precipitation at the PPS between September 2013 and August 2014 (grey bars) and multiannual (1978–2014) average of precipitation totals (black bars) (Kępski *et al.* 2013; Łaszyca *et al.* 2014).

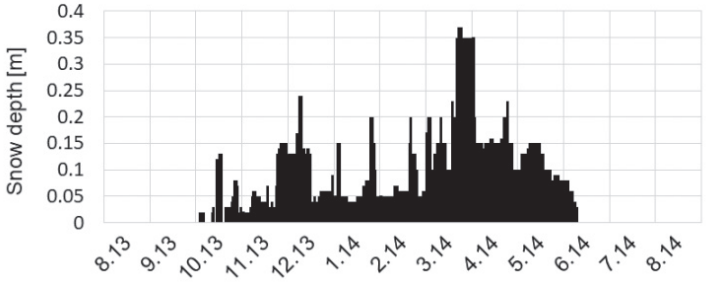

Fig. 3. Snow depth from October 2013 to June 2014 measured at the Polish Polar Station Hornsund modified after Kępski *et al.* (2013) and Łaszyca *et al.* (2014).

the beginning of meteorological observations at PPS (Table 1) (Kępski *et al*. 2013; Łaszyca *et al*. 2014).

Days with strong winds were considerably frequent in the ablation season 2014 but the mean wind speed was higher during the accumulation than the ablation season (Table 1). Those winds were prevailing from the eastern sector as in most Svalbard areas (Førland *et al*. 1997; Jaedicke and Gauer 2005).

The lowest temperature on Hansbreen occurred over the highest parts of the glacier (T9) but occasionally the inversion of temperature was noticed showing lowest temperature over lower parts of Hansbreen (Fig. 4). The temperature difference between glacier and PPS was noticable. The negative temperature on Hansbreen occurred earlier (23 days) than at the PPS and the new seasonal snow cover in elevated parts of the glacier may appear in September.

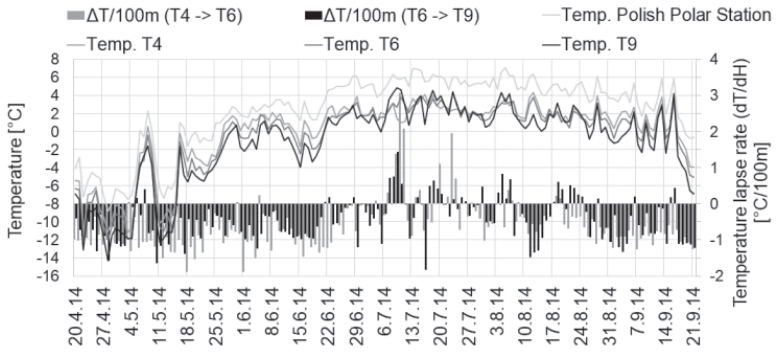

Fig. 4. Daily air temperature at automatic weather stations (H4, H6 and H9) on Hansbreen and at the Polish Polar Station Hornsund, temperature lapse rates between reference sites (ΔT) during the 2014 ablation season.

Data and methods

Snow depth. — Snow depth on the glacier was measured using a Ground Penetrating Radar (GPR) system, which produces images of the subsurface structure based on differences of the dielectric properties of the materials penetrated by the radar waves (Grabiec *et al*. 2011), allowing to identify distinct internal boundaries. The GPR survey was conducted using a common offset survey mode over several surface profiles within an area of Hansbreen accessible in April 2014 (Fig. 5), around the maximum snow accumulation period. The GPR system used an 800 MHz shielded antenna with a vertical resolution of 6.5 cm (1/4 of the wavelength) (Sheriff 1977; Grabiec *et al*. 2011).

The GPR system was mounted onto a sledge pulled by a snowmobile and the astern GPR antenna loaded into pulkas. The average distance interval between consecutive traces was approximately 1 m, which resulted from the speed of the snowmobile (*ca*. 20 km h^{-1}) and the trigger time internal (0.2 s). The data was georeferenced using a GPS receiver working in a differential kinematic mode. The snow depth was measured through profiles amounting to *ca*. 110 km of total length (Fig. 5). The validation of results of radar soundings by ablation stakes readings is shown in (Fig. 8 and Table 4). The standard deviation of identification of the snow-ice interface in the ablation area is 0.43 ns, whereas in the accumulation zone of Hansbreen it might be *ca*. 50% larger (Grabiec 2017).

The snow depth data derived from the GPR survey provides semi-linear information. In order to obtain a reliable spatial pattern of snow distribution for the entire glacier, we compared four methods of data interpolation: Inverse Distance Weight, Kriging, Spline and Natural Neighbourhood. Based on a cross-validation (rotation estimation) (Kohavi 1995; Browne 2000), the Inverse Distance Weights (IDW) was finally chosen with a mean square error of 0.041 m, which value was the lowest among the compared methods. IDW was used for the further interpolation to a 100 m grid resolution.

Snow density. — The snow depth and density of snowpack are components of calculation the SWE. The SWE from the end of accumulation season (EAS) was calculated based on snow depth measurements by GPR (Fig. 9a, made on 20.04.2014) and density survey in three spring snow pits (Fig. 1, Table 2) made on 5/6.05.2014.

We found that the bulk snow density values increase with snow depth. Based on snow depth to density relationship and snow distribution (Fig. 5), the snow density field over Hansbreen in EAS has been calculated (Fig. 6).

In the ablation period, the meltwater starts to percolate into deeper layers in the snowpack. Part of this water remains in the snow cover due to refreezing, until the melting point is reached, or as capillary water, increasing its density, while remaining water drains away to the glacier. We assumed that the density

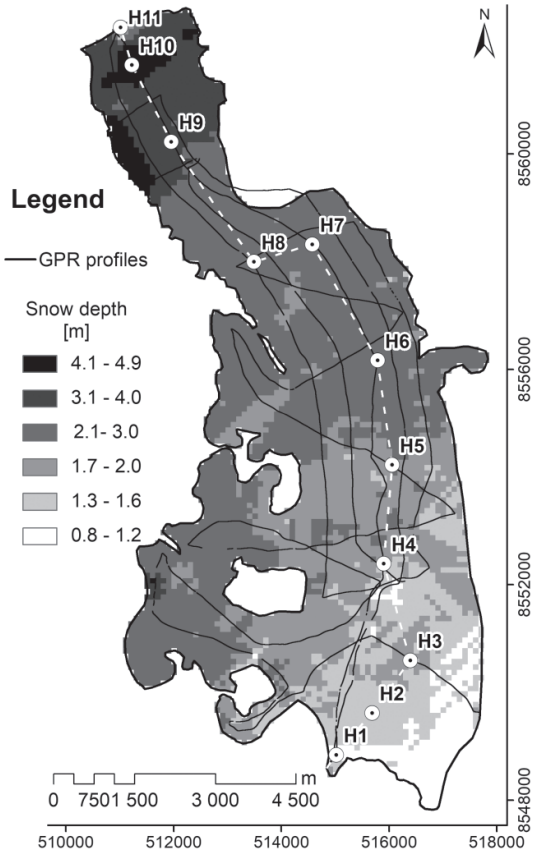

Fig. 5. Snow depth surveyed by Ground Penetrating Radar on the 12th April 2014 on Hansbreen (black solid line). White dashed line denotes longitudinal profile across the ablation stakes H1–H11; see Fig. 8 for details.

of the snowpack increases proportionally to the amount of meltwater, while melting can be explained by the sum of positive degree days (PDD).

The change of the snowpack density ($\Delta\varrho_i$) due to percolation of meltwater was calculated in three steps. Firstly, we have computed the overall change of snow densities between snow pits made at the end of the accumulation season (5/6.05.2014) (ϱ_{acc}) and on 13.06.2014 (ϱ_{est}) at H4 [1]. In the second step the change of snow densities obtained in step [1] have been divided by the PDD sum (5/6.05.2014 – 13.06.2014) in order to calculate the snow density index (x) [2] which reached 5.31 kg m^{-3} for every 1°C. Finally in the third step, we have calculated the density increment depending on positive temperature in specific day (T_i^+) [3] using the same snow density index for H4, H6 and H9. Based on earlier observations (Laska *et al*. 2016, 2017b), we assumed maximum average density of snowpack during ablation season reaching 530 kg m^{-3} till the end

Table 2

Basic characteristics of snow density derived from snow pits on Hansbreen. The UTM zone 33N geodetic system and WGS (1984) datum was used.

Location	Date of measurement	Snow density at the end of accumulation season ϱ_{acc} [kg m^{-3}]	Estimated summer snow density ϱ_{est} [kg m^{-3}]	Snow depth [m]	Elevation [m a.s.l]	Northing	Easting
H4	5.5.2014	374	530	1.60	175	8 552 094	515 890
H6	5.5.2014	399	530	2.10	269	8 556 142	515 805
H9	6.5.2014	466	530	2.78	406	8 560 230	511 955

of June 2014 (Fig. 7). The gradually increase of snow density was applied for whole glacier and next the maximum snow density (530 kg m^{-3}) defined snow density for remaining part of ablation season.

$$\Delta\rho_i = \begin{cases} \Delta\rho = \rho_{est} - \rho_{acc} & (1) \\ x = \frac{\Delta\rho}{PDD_n} & (2) \\ \Delta\rho_i = x \cdot T_i^+ & (3) \end{cases}$$

where: n – number of days, i – specific day counted from the beginning of the melting period.

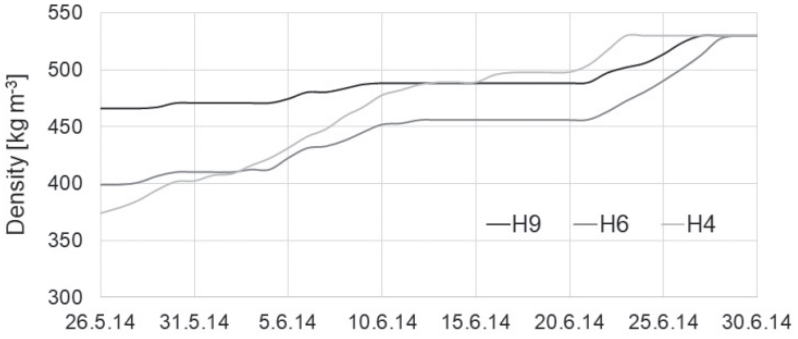

Fig. 6. Evolution of snow density on Hansbreen from the beginning of snowmelt (26.05.2014) to the end of June (30.06.2014) at 3 locations (H4, H6 and H9) according to formulas 1–3.

Table 3

The degree day factor (DDF) index [m d^{-1} °C^{-1}] and DDF gradient (ΔDDF/100m) based on stakes readings (H4, H6 and H9).

Date	DDF H4 (187 m a.s.l)	DDF H6 (278 m a.s.l)	DDF H9 (424 m a.s.l)	ΔDDF/100m (below H6)	ΔDDF/100m (above H6)
20.4 – 20.6.2014	0.026	0.035	0.077	0.011	0.029
20.6 – 15.7.2014	0.023	0.018	0.015	-0.006	-0.002
15.7 – 22.8.2014	–	0.017	0.010	–	-0.005
22.8 – 21.9.2014	–	–	0.006	–	–

The changes of snow density in the melting period have been estimated at sites H4, H6 and H9 in one day time step (Fig. 6). At each calculation step, the snow depth-to-density conversion formula was used (procedure similar as at EAS) and applied to set up the density field over Hansbreen. The snow density has increased by 146 kg m^{-3} (H4 site), 131 kg m^{-3} (H6 site) and 79 kg m^{-3} (H9 site) till the end of June.

Snow water equivalent. — SWE derived from the snow deposited in winter and melted during summer was calculated using the following equation after Sturm *et al*. (2010):

$$SWE = h_s \frac{\rho_b}{\rho_w} \tag{4}$$

where the snow depth (h_s) was measured in meters, the bulk snow density (ϱ_b) in kg m^{-3} and the density of water (ϱ_w) is 1000 kg m^{-3}.

Air temperature field over Hansbreen. — Air temperature was measured at three automatic weather stations located on Hansbreen at different altitudes (H4 – 187 m a.s.l, H6 – 278 m a.s.l and H9 – 424 m a.s.l., Fig. 1). The temperature data were used to calculate the vertical temperature gradient for every day during the ablation season (Fig. 4). The analysis of the temperature lapse rate (ΔT/ΔH) allows to identify thermal inversions taking place mainly in summer. The thermal inversion in ablation season occurred in 20 and 36 days (at H4–H6 and H6–H9 profiles, respectively) (Fig. 4). The average temperature lapse rates at H4–H6 and H6–H9 were -0.61 and -0.44, respectively.

Daily mean temperature and the temperature lapse rate between reference sites on the glacier, were used to extrapolate the temperature to every grid cell of Hansbreen digital elevation model (DTM) based on SPOT images taken in 2008 (Korona *et al*. 2009).

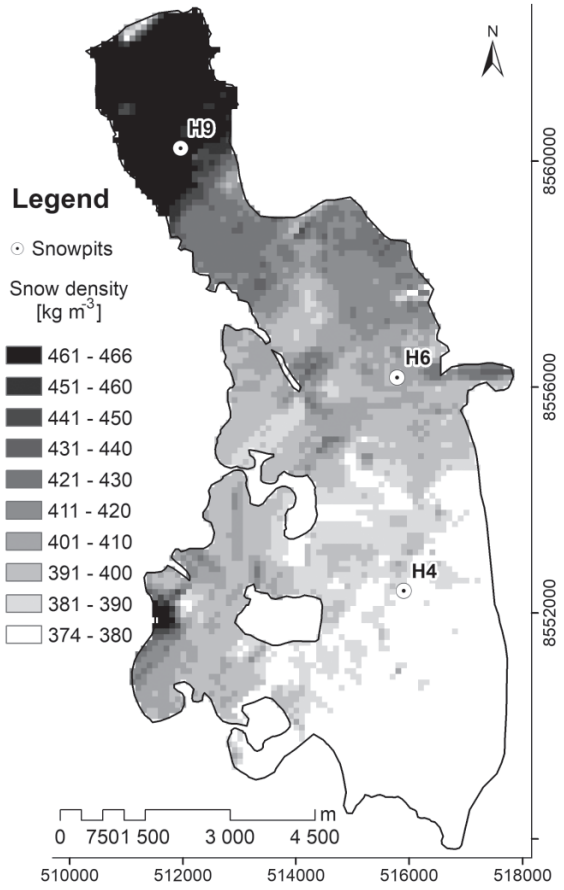

Fig. 7. Distribution of average snow density for the maximum accumulation period in 2014 on Hansbreen.

Temperature Index Model. — Due to the apparent impact of air temperature on snow ablation, Temperature Index Model (TIM) arises as a powerful tool to approximate snowmelt (*e.g.*, Braithwaite 1985; Hock 2003). TIM uses DDF as a relationship between overall snow ablation (a_{snow}) and sum of the positive daily means of air temperature (T^+) taking place within the same period (expressed in days – n) as snow ablation measurements (Hock 2003):

$$DDF = \frac{H_a}{\sum_{i=1}^{n} T^+} \tag{5}$$

In this study, the snowmelt was calculated based on ablation stakes readings (H4, H6 and H9). Due to spatially fickle snow properties and atmospheric conditions, we apply variable DDF values (Ismail *et al*. 2015) across the study area.

Results

Degree Day Factor. — The DDF was calculated for reference sites (in H4, H6 and H9) in different periods. In the next step the DDF gradient (**Δ**DDF/100m) between reference sites was computed. Finally, the DDF field was calculated based on changes of DDF with altitude and glacier DEM in a specific time period (Table 3).

The average seasonal DDF values for each zone were: 0.025, 0.023 and 0.027 m d^{-1} $°C^{-1}$ for the H4, H6 and H9, respectively. The DDF was considerably higher in the first period analysed (20.04.2014 – 20.06.2014) compared to the others (Table 3). Despite negative daily average temperature in this period in some days the snowmelt may occur as a result of positive maximum temperature. This days are not included in PDD although they influence on total ablation, and in consequence overstate DDF index. The melt rate was calculated for each grid cell over Hansbreen for every day during the summer, based on the DDF values (Table 3).

Distribution of snow cover in the 2014 spring and summer season. — Snow depth in the 2013/2014 winter season increases with elevation as a result of more frequent and efficient snow precipitation in higher parts of the glacier and the decrease of temperature with altitude (Fig. 5). The shallowest snow cover is present in the lowermost, south-eastern part of Hansbreen, where it does not exceed 1.0 m, reaching a minimum of 0.8 m on the front of glacier. The deepest snow cover occurred in the northern and north-western the parts of the glacier, with maximum depth of 4.9 m (Fig. 5).

Based on the assumption that the DDF values differ among glacier zones, we identyfied the rate of snow ablation and snow depth thinning along the entire glacier (Fig. 8). In the frontal part of the glacier, the snow cover declined by the end of June, as a result of the small snow cover depth and fast snowmelt rate (0.025 m d^{-1} $°C^{-1}$) compared to that from the other parts of the glacier (Fig. 8).

Due to application of DDF variable in space and time, the snow depth at the beginning of the ablation period calculated in the model fits well with the data acquired at the reference stakes (Table 4). However, there are still some discrepancies between the modelled and measured data for the H4 and H6 sites, due to the difference in dates of GPR survey and the stakes reading (12 and 20.04.2014) (Fig. 8 and Table 4).

The absolute difference between both data ranged from 0 to 0.45 m (0–16.5%). The largest errors have been noted at stakes located in accumulation area (H8 and H11), whereas snow depth at stakes in the ablation area shows considerably good agreement with radar data (absolute error lower than 0.1 m or 5%). The best matching was obtained for the middle part of Hansbreen, between the H4 and the H9 ablation stakes.

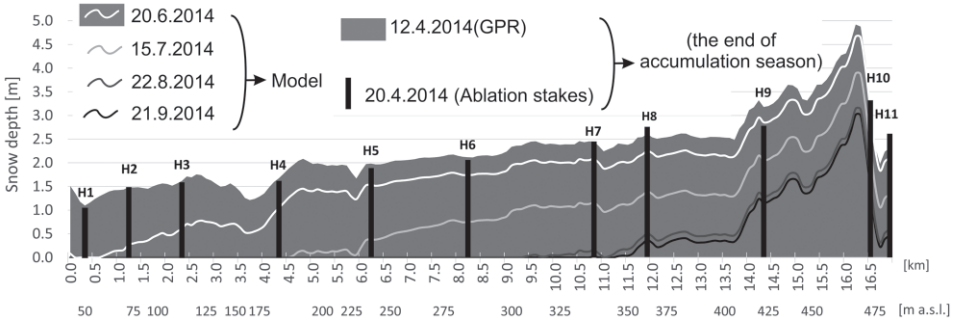

Fig. 8. Snow depth from a temperature index model following the longitudinal profile shown in Fig. 5.

The H8 stake was located approximately at the Equilibrium Line Altitude (ELA), where superimposed ice within the snowpack may occur, hindering a clear identification of the snow cover/glacier ice interface. Significant discrepancies between the modelled snow depth and the data recorded at the ablation stakes are observed at the lowermost and the highest parts of Hansbreen. These results were expected in areas where DDF was extrapolated beyond the elevation range of stakes used to estimate this factor (H4, H6 and H9). For these areas of the glacier, the DDF may not be valid, increasing the uncertainties of the modelled snow depth.

Winter mass balance and water production from snowmelt. — The point winter mass balance (b_w) expressed in SWE and its glacier-wide distribution (B_w – Fig. 9A) was derived from snow density pattern (Fig. 7) and the snow depth field over Hansbreen in spring 2014 (Fig. 5). The winter balance (B_w) has been calculated as 0.88 m w.e. in relation to B_w = 0.94 m w.e. referred in WGMS. B_w generally increase with the elevation subsequently following changes of snow depth and density and ranging between 0.28 m w.e. in the lowest parts and 2.36 m w.e. in the highest parts of the studied glacier (Fig. 9A).

In order to estimate how much water is produced from snow melting during the summer season, we used the TIM model over entire glacier (Fig. 9B). In the upper parts of the glacier, over 330 m a.s.l. in the NE part of Hansbreen and 350 m a.s.l. in the N and NW parts, the winter mass balance exceeds the snow ablation (Fig. 9 and Fig. 10A). Similar features occur over 400 m a.s.l. in the western tributary glaciers: Deileggbreen, Tuvbreen and Staszelisen (Fig. 9 and Fig. 10A). In the 24.2% of Hansbreen's surface area, the snow cover did not completely melted out during the summer season, thus it makes up a surplus of the snow balance (compare to Fig. 8 and Fig. 10A). Consequently, the area without snow at the end of the ablation season covers more than three-fourth of the whole glacier surface.

Table 4

Snow depth on 20.04.2014 based on Ground Penetrating Radar (GPR) survey and stakes reading; snow ablation [m] from model and recorded from stakes (for specific dates: 20.06, 15.07, 22.08 and 20.09.2014) on Hansbreen. As a reference stakes H4, H6, H9 (see Table 3).

No. of Stakes			H1	H2	H3	H4	H5		H6	H7	H8	H9	H10	H11	Root mean square error
Initial snow depth at the end of accumulation season	20.4.2014	stakes[1]	1.05	1.49	1.59	1.62	1.89		2.06	2.45	2.76	2.73	3.32	2.61	
		GPR	1.10	1.49	1.62	1.69	1.98		2.12	2.45	2.61	3.18	3.27	2.31	
		GPR – stakes	0.05 (4.8%)	0.00 (0%)	0.03 (1.9%)	0.07 (4.3%)	0.09 (4.8%)		0.06 (2.9%)	0.00 (0%)	-0.15 (-5.4%)	0.45 (16.5%)	-0.05 (-1.5%)	-0.30 (-11.5%)	
Snow ablation [m w.e.]	20.6.2014	stakes[1]	0.78	–	0.66	0.61	0.52		0.38	0.42	0.50	0.33	0.45	0.37	
		model	1.10	1.17	0.97	0.60	0.47		0.37	0.38	0.36	0.33	0.24	0.21	
		model – stakes	0.31 (40%)	–	0.31 (47%)	-0.01 (-.6%)	-0.05 (-9.6%)		-0.01 (-2.6%)	-0.04 (-9.5%)	-0.14 (-28%)	0.00 (0%)	-0.21 (-46.7%)	-0.16 (-43.2%)	0.20
	15.7.2014	stakes[1]	–	–	–	1.62	1.02*	(1.89)	1.37	1.29	(1.47)	1.12	1.49	1.13	
		Model	1.10	1.49	1.61	1.69	1.08*	1.61	1.36	1.30	1.23	1.13	1.02	0.99	
		model – stakes	–	–	–	0.07 (4.3%)	0.06* (5.9%)*	(-0.28) (-14.8%)	-0.01 (-.7%)	0.01 (.8%)	(-0.24) (-16.3%)	0.01 (.9%)	-0.47 (31.5%)	-0.14 (-12.4%)	0.27
	22.8.2014	stakes[1]	–	–	–	–	1.89		2.06	2.28	(2.29)	1.88	2.35	2.36	
		model	–	–	–	–	1.96		2.11	2.44	2.12	1.89	1.76	1.73	
		model – stakes	–	–	–	–	0.07 (3.7%)		0.05 (2.4%)	0.16 (7%)	(-0.17) (-7.4%)	0.01 (.5%)	-0.59 (-25.1%)	-0.63 (-26.7%)	0.4

Table 4. Continued

No. of Stakes			H1	H2	H3	H4	H5	H6	H7	H8	H9	H10	H11	Root mean square error
	21.9.2014	stakes[1]	–	–	–	–	–		2.33	(2.76)	2.01	2.26	2.48	
		model	–	–	–	–	–	2.11	2.44	2.26	2.02	1.89	1.85	
		model – stakes	–	–	–	–	–		0.11 (4.7%)	(-0.50) (-18.1%)	0.01 (.5%)	-0.37 (-16.3%)	-0.63 (-25.4%)	0.45

* date of observation 05.07.2014; ( ) uncertain data

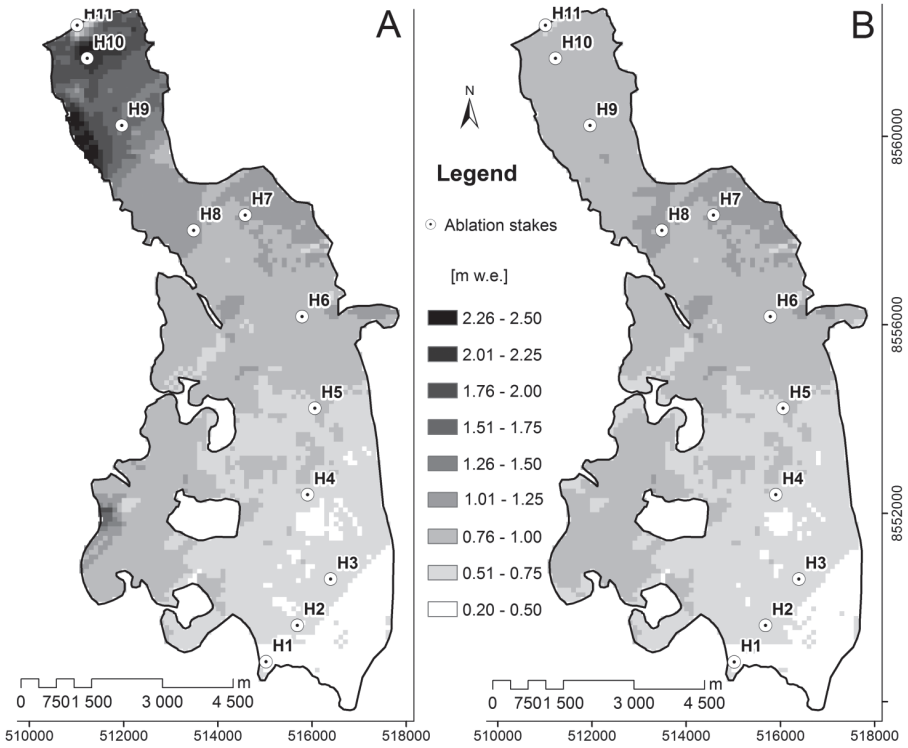

Fig. 9. Glacier-wide winter mass balance in 2013/2014 (**A**) and snow ablation in 2014 (**B**). Note that snow ablation have to be expressed in negative values.

Most of the meltwater from snow cover was produced in the middle part of Hansbreen (area around H7 and H8, Fig. 9B), as the combined impact of favourable thermal conditions, snow depth and ablation rate. In this part of the glacier, the snowmelt provides a maximum of 1.17 m w.e. (Fig. 9B). Above this zone snow ablation is rather constant and remains in range of 0.75–1.00 m w.e. Downslope from the maximum snowmelt zone, water production decreases reaching its minimum (0.26 m w.e.) in the south-eastern part of Hansbreen (Fig. 9B). In this area the remaining energy available in summer for ablation was consumed for ice melting, which is not included in this study.

The most intensive release of water from the snowpack took place between the end of June and the first half of August 2014 (Fig. 11A). There were six events of snowmelt recorded, exceeding 0.02 m w.e. daily, with a maximum value of 0.024 m w.e. on 15.07.2014. The average glacier-wide daily production of meltwater from the snow cover in 2014 ablation season period was 0.006 m w.e. The cumulative ablation (Fig. 11B) shows that in summer 2014 $43.97 \cdot 10^6$ m^3 (0.77 m w.e.) of meltwater has been produced, 87 % of which till the 1st August.

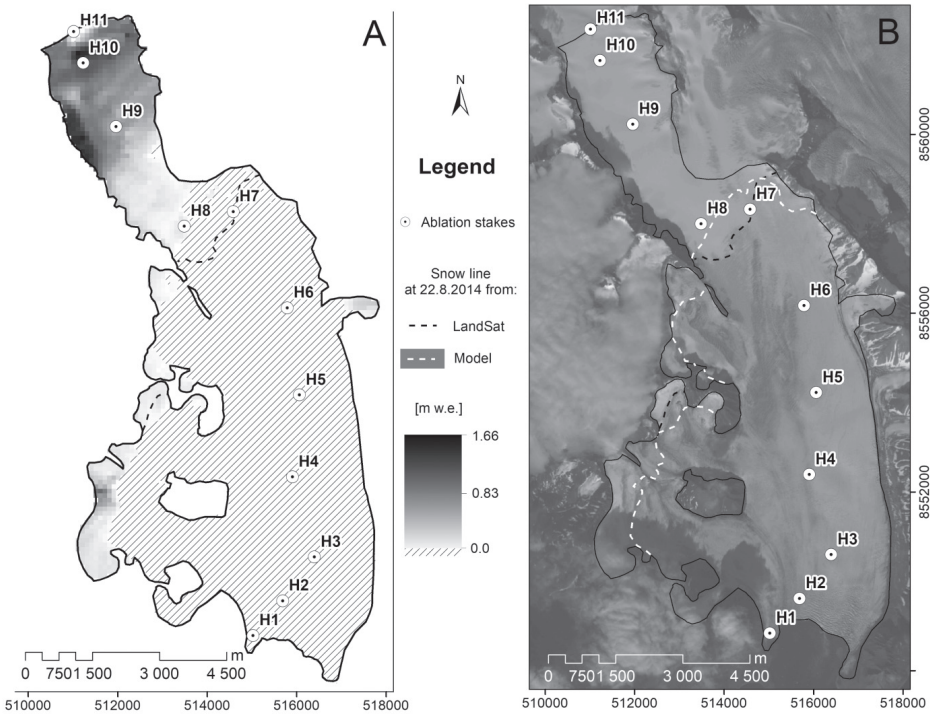

Fig. 10. Snow balance (SWE) calculated at the end of the ablation season on 21.9.2014 (**A**) and panchromatic Landsat 8 images from 22.8.2014 (**B**).

Discussion

Despite of numerous meteorological factors influencing on melt rate of snow cover, *i.e*. wind speed, total precipitation, relative humidity and total radiation, the air temperature is the most significant (Migała *et al*. 2006). Thereby, the TIM approach used here allows to estimate snow net balance ($B_{n(snow)}$). Moreover, application of DDF variable in space and time may improve results of snow balance estimations comparing with the constant DDF factor. In general, the snow ablation rate and total meltwater production depend on the atmospheric conditions and their fluctuations in the specific year. Hence, using the same DDF for subsequent years is limited due to variations in albedo, surface energy balance and others meteorological factors (Migała *et al*. 2006) and may generate serious mass balance errors (Van den Broeke *et al*. 2010).

The validation of radar sounding results by ablation stakes readings shows some differences in snow depth at the end of the accumulation season (Fig. 8 and Table 4). Spatially variable range of discrepancies between observed snow depth and derived from radar sounding are in accordance with distribution

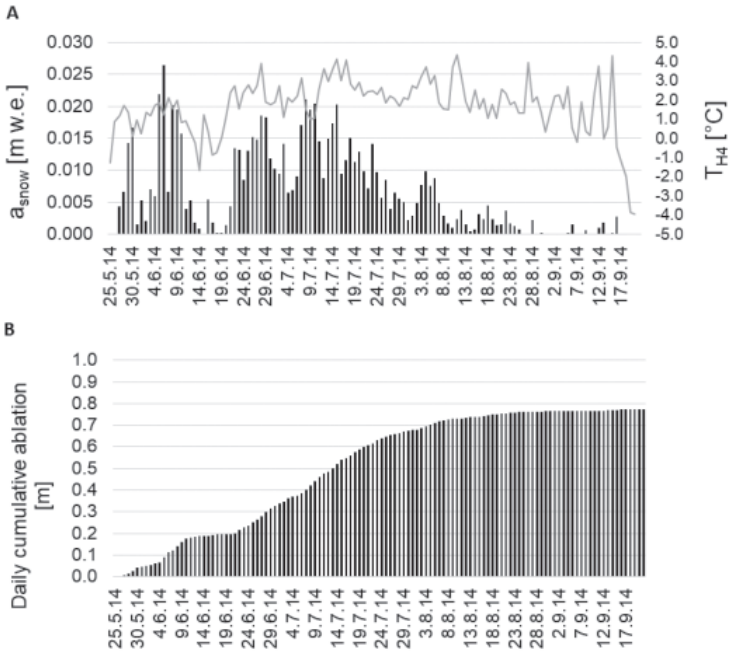

Fig. 11. Meltwater production in summer season 2014 on Hansbreen. Daily ablation (**A**) and cumulative ablation (**B**). The mean daily temperature at H4 is marked as a grey line.

of uncertainties of delimitation of ice-snow interface from GPR data along glacier centreline 0.053 m after Grabiec (2017). Larger difficulties in correct identification of snow depth from radio-echo sounding profiles above ELA result from lower contrast in dielectric properties between snow and underlying firn or superimposed ice than between snow and ice as occur in ablation zone. Besides identification errors described above, vertical resolution and variations in radio wave velocity may influence on accuracy of snow depth derived from radio-echo sounding. Observed discrepancies may also come from one week difference in both surveys and *ca*. 10 m distance between measurement stakes and GPR track (Fig. 8 and Table 4).

Based on the observed snow distribution and density pattern we estimated SWE in every grid (100 × 100 m) for entire Hansbreen. However, the data interpolation ignores the variations of snow depth occurring at a scale of less than the 100 m grid, which gives some uncertainty to the general estimation. Likewise, the use of snow density pattern, based on the average of the entire snow profile, had an influence on overestimation of $B_{n(snow)}$, especially in the elevated part of Hansbreen where only upper and less dense snow layers were

melted. However, during the ablation season, due to water percolation in the snow cover, the snow density distribution in snow columns became more homogenous.

The snow line observed on the Landsat 8 panchromatic image (Fig. 10) on 22 August 2014 was compared with the modelled one showing total underestimation of snow range by 3.22 km^2 at the end of summer, representing 6% of the entire glacier area. In the western part of the glacier, this underestimation reached 3.94 km^2 (7.3%), whereas in the northern part of glacier the model was overestimated by 0.72 km^2 (1.3%). Moreover, the altitude of the modelled snow line and retrieved from Landsat image differs by *ca*. 20 m in the north (mainly overestimation) and *ca*. 90 m in the west (mainly underestimation).

The extent of snow cover remaining at the end of the ablation season (21.09.2014) was compared to the snowline derived from closest available Landsat 8 image, taken on 22nd August 2014 (Fig. 10). The difference between those two limits is substantial and ranging from 0.2 km in NW part of Hansbreen main stream, to up to 1.2 km in NE sector of the glacier. The discrepancies in snow extent can be partly explained by more than one month difference between taking the satellite image and the end of the ablation season. When comparing Landsat based snow line with snow extent modelled on the same date (22.08.2014), the inconsistency is considerably smaller, *ca*. 0.6 m on average (Fig. 10B).

The inconformity in the snow line extent between the model and the satellite image can be partly explained by the shift in the dates of actual snow accumulation maximum and the GPR survey conducted seven days earlier (Fig. 8). Furthermore, factors such as wind speed and direction influence on snow re-deposition, particularly during and shortly after each precipitation event, may modify initially deposited snow (Grabiec *et al*. 2006, 2011; Grabiec 2017; Laska *et al*. 2017a, 2017b).

A detailed analysis of the dynamics of snowmelt in 2014 on all tidewater glaciers terminating into Hornsund derived from Landsat 8 images were presented by Laska *et al*. (2017b). Based on the image from 20.08.2014, they calculated snow free area on Hansbreen at 65.4%, while in this paper it was 71.5%. The difference is the most pronounced in the eastern part of the glacier, below the ELA. The inconsistency in both studies can be explained by application of individual data processing methods and interpretation ways. Laska *et al*. (2017b) used supervised classification to separate limits and included superimposed ice in the *snow* class, as an accumulation component. In this study, the snow line was recognized and drawn manually and considered classically as located above superimposed ice zone. It can be concluded that the *ca*. 6% surface area resulting from the difference in both studies originates from the superimposed ice.

The differences in snow depth and surface mass balance between stake readings and the modelling (Fig. 8, Table 4 and 5) are also noticeable. The modelled B_w underestimates the multiannual average at stakes by 0.09 and

Table 5

Mass balance components on Hansbreen. Winter balance – Bw, Summer Snow Ablation – As(snow), Summer Balance – Bs, Snow Net Balance – Bn(snow) and Net Mass Balance – Bn*.

Date	Method	B_w [m w.e.]	$A_{s(snow)}$ [m w.e.]	B_s [m w.e.]	$B_{n(snow)}$ [m w.e.]	B_n^* [m w.e.]
2013/2014	Model (TIM)	0.88 ± 0.12	-0.77 ± 0.29	–	0.11 ± 0.31	–
	Ablation Stakes[4]	0.94	-0.78	-1.21	0.16	-0.27
Multiannual average	Ablation stakes WGMS monitoring (1989–2016)[1–5]	0.97	–	-1.26	–	-0.28
	Total mass balance** (2000–2008)[6]	–	–	–	–	-0.8

* including ice melting; ** including ice melting and calving
[1] Szafraniec (2002); [2] WGMS (2012); [3] WGMS (2015); [4] Błaszczyk *et al.* (2019a); [5] Grabiec *et al.* (2012); [6] Oerlemans *et al.* (2011)

0.06 in 2014 (Table 5). The problems associated with the snow-firn interface delimitation from the GPR data over accumulation zones of glaciated areas in southern Spitsbergen have been widely discussed by Laska *et al.* (2017a) and Grabiec (2017).

The uncertainty range of TIM model is considerable (Table 5). Particularly large error in the modelled $B_{n(snow)}$ come from overlapping errors arising at each measurement and processing step, including: GPR profiling, data interpolation, density pattern, and definition of temperature and ablation fields.

The modelled snow balance components in 2014 were compared to the mass balance calculated from the classical stakes monitoring and show accordance within uncertainty range of modelling (Table 5). The winter accumulation is insufficient to keep the overall surface mass budget in balance. However, snow cover, due to its reflective properties, *i.e.* relative high surface albedo, may considerably control rate of summer ablation. Detailed analysis of the mass balance components in period 1989–2016 have shown that the years with the highest values of the summer mass balance (*e.g.*, -1.88 m w.e. in 2001) are strongly correlated to minimum values of winter mass balance (0.78 m w.e. in 2001). Moreover, snow cover contributes substantially to the meltwater production. In 2014, snowmelt was responsible for more than 64% of summer balance (B_s). However, even if snow cover is not a dominating source of the meltwater in summer, it have strong impact on summer and net mass balance.

Conclusion

This paper presents results of modelling snow net balance on Hansbreen based on spatial distribution of snow depth and its density. The field observations show correlation between snow density and snow cover depth. We used this relation to define a pattern of snow density for the entire glacier, which reached in the end of accumulation season its maximum value of 466 kg m^{-3} in the highest parts of Hansbreen, its minimum reaching 374 kg m^{-3} in the frontal part of the glacier and the average snow density of 402 kg m^{-3}. During ablation season, we used gradual densification of snow reaching the maximum till the end of June at 530 kg m^{-3} for the entire glacier. To this end, we applied DDF changes along the glacier surface as a continuous parameter changing with altitude. In this case, the average seasonal DDF values for the reference ablation stakes H4, H6 and H9 were 0.025, 0.023 and 0.027 m d^{-1} $°C^{-1}$, respectively and 0.025 m d^{-1} $°C^{-1}$ on average for whole glacier.

We used the field observations and estimations based on TIM to assess the snow net balance in 2013/2014 on Hansbreen. The B_w was estimated to be 0.88 m w.e., whereas the average daily water production from the snowmelt was 0.0065 m w.e. Our results show that the snow balance is insufficient to cover the mass loss during summer season. Snowmelt during the 2014 ablation season gave 0.77 m w.e. ($41.52 \cdot 10^6$ m^3 of freshwater in total) being an 85.5% of total water accumulated during winter in the snow cover. The snow completely melted from 75.8% of the surface of Hansbreen in 2014.

Acknowledgements. — This research has been supported by the following projects: *Arctic climate system study of ocean, sea ice and glaciers interactions in Svalbard area* – AWAKE2 (Pol-Nor/198675/17/2013) granted by the National Centre for Research and Development within the Polish-Norwegian Research Cooperation Programme and the National Science Centre PRELUDIUM 4: *Role of meltwater from snow cover for supplying drainage systems of the Spitsbergen glaciers* (2012/07/N/ST10/03784). Glaciological, hydrological and meteorological data have been processed under assessment of the University of Silesia data repository within project Integrated Arctic Observing System (INTAROS). INTAROS project has received funding from the European Union's Horizon 2020 research and innovation programme under grant agreement No 727890. The authors wish to thank the various national institutions and persons who helped directly support this publication. The Institute of Geophysics Polish Academy of Sciences (IG PAS) granted access to the glacier mass balance data, meteorological data and reference GPS data. We would like to thank Michał Pętlicki (IG PAS) for providing detailed data from mass balance monitoring and support. The Polish Polar Station Hornsund ensured logistic facilities during the field campaign. The snow profile from ablation season (13.06.2014) were made by Daniel Kępski. The Data from automatic weather station (Hansbreen) were provided by Tomasz Budzik (University of Silesia). The authors would like to thank Jacek Jania for the constructive discussion of the paper. This publication has been financed from the funds of the Leading National Research

Centre (KNOW) received by the Centre for Polar Studies for the period 2014–2018. We would like to thank two anonymous reviewers for valuable comments and apt comments that helped improving this work.

References

Aas K.S., Dunse T., Collier E., Schuler T.V., Berntsen T.K., Kohler J. and Luks B. 2016. The climatic mass balance of Svalbard glaciers: a 10-year simulation with a coupled atmosphere–glacier mass balance model. *The Cryosphere* 10: 1089–1104.

Benn D.I. and Evans D.J.A. 2010. *Glaciers and Glaciation*. Hodder Education. London, UK: 802 pp.

Błaszczyk M., Jania J. and Hagen J.O. 2009. Tidewater glaciers of Svalbard: Recent changes and estimates of calving fluxes. *Polish Polar Research* 30: 85–142.

Błaszczyk M., Jania J.A. and Kolondra L. 2013. Fluctuations of tidewater glaciers in Hornsund Fjord (Southern Svalbard) since the beginning of the 20th century. *Polish Polar Research* 34: 327–352.

Błaszczyk M., Ignatiuk D., Uszczyk A., Cielecka-Nowak K., Grabiec M., Jania J.A., Moskalik M. and Walczowski W. 2019a. Freshwater input to the Arctic fjord Hornsund (Svalbard). *Polar Research* 38: 3506.

Błaszczyk M., Ignatiuk D., Grabiec M., Kolondra L., Laska M., Decaux L., Jania J., Berthier E., Luks B., Barzycka B. and Czapla M. 2019b. Quality assessment and glaciological applications of digital elevation models derived from space-borne and aerial images over two tidewater glaciers of southern Spitsbergen. *Remote Sensing* 11: 1121.

Braithwaite R.J. 1985. Calculation of degree-days for glacier-climate research. *Zeitschrift für Gletscherkunde und Glazialgeologie* 20: 1–8.

Braithwaite R.J. 1995. Positive degree-day factors for ablation on the Greenland ice sheet studied by energy-balance modelling. *Journal of Glaciology* 41: 153–160.

Braithwaite R.J. and Olesen O.B. 1989. Calculation of glacier ablation from air temperature, West Greenland. *In*: J. Oerlemans (ed.) *Glacier Fluctuations and Climatic Change*. *Glaciology and Quaternary Geology* 6: 219–233.

Brandt O., Kohler J. and Lüthje M. 2008. Spatial mapping of multi-year superimposed ice on the glacier Kongsvegen, Svalbard. *Journal of Glaciology* 54: 73–80.

Browne M.W. 2000. Cross-validation methods. *Journal of Mathematical Psychology* 44: 108–132.

Bruland O., Liston G.E., Vonk J., Sand K. and Killingtveit Å. 2004. Modelling the snow distribution at two high arctic sites at Svalbard, Norway, and at an alpine site in central Norway. *Hydrology Research* 35: 191–208.

Carroll D., Sutherl, D.A., Shroyer E.L., Nash J.D., Catania G. and Stearns L.A. 2015. Modeling turbulent subglacial meltwater plumes: implications for fjord-scale buoyancy-driven circulation. *Journal of Physical Oceanography* 45: 2169–2185.

Christensen J.H., Hewitson B., Busuioc A., Chen A., Gao X., Held R., Magaña Rueda V., Mearns L., Menéndez C.G., Raisanen J., Rinke A., Sarr A. and Whetton P. 2007. Regional climate projections. *In*: S. Solomon, D. Qin, M. Manning, Z. Chen, M. Marquis, K.B. Averyt, M. Tignor and H. L. Miller (eds) *Climate Change 2007: The Physical Science Basis*. Contribution of Working group I to the Fourth Assessment Report of the Intergovernmental Panel on Climate Change, Cambridge University Press, Cambridge: 847–940.

Cowan E. 1992. Meltwater and tidal currents: controls on circulation in a small glacial fjord. Estuarine. *Coastal and Shelf Science* 34: 381–392.

DAI A. 2008. Temperature and pressure dependence of the rain-snow phase transition over land and ocean. *Geophysical Research Letters* 35: L12802.

DECAUX L., GRABIEC M., IGNATIUK D. and JANIA J. 2019. Role of discrete water recharge from supraglacial drainage systems in modeling patterns of subglacial conduits in Svalbard glaciers. *The Cryosphere* 13: 735–752.

FOUNTAIN A.G. 1989. The storage of water in, and hydraulic characteristics of, the firn of South Cascade Glacier, Washington State, USA. *Annals of Glaciology* 13: 69–75.

FOUNTAIN A.G. 1996a. Effect of snow and firn hydrology on the physical and chemical characteristics of glacial runoff. *Hydrological Processes* 10: 509–521.

FOUNTAIN A.G. 1996b. The storage of water in, and hydraulic characteristics of the firn of South Cascade Glacier, Washington State, USA. *Annals of Glaciology* 13: 69–75.

FØRLAND E.J., HANSSEN–BAUER I. and NORDLI P.Ø. 1997. Climate statistics and longterm series of temperature and precipitation at Svalbard and Jan Mayen. *DNMI Det Norske Meteorologiske Institutt*, Report No. 21/97 KLIMA: 72 pp.

FØRLAND E.J. and HANSSEN-BAUER I. 2003. Past and future climate variations in the Norwegian Arctic: overview and novel analyses. *Polar Research* 22: 113–124.

FUJITA K. 2008. Effect of precipitation seasonality on climatic sensitivity of glacier mass balance. *Earth and Planetary Science Letters* 276: 14–19.

GRABIEC M. 2005. An estimation of snow accumulation on Svalbard glaciers on the basis of standard weather-station observations. *Annals of Glaciology* 42: 269–276.

GRABIEC M. 2017. *The state and contemporary changes of glacial systems in southern Spitsbergen in the light of radar methods*. Wydawnictwo Uniwersytetu Śląskiego, Katowice: 328 pp. (in Polish)

GRABIEC M., LESZKIEWICZ J., GŁOWACKI P. and JANIA J. 2006. Distribution of snow accumulation on some glaciers of Svalbard. *Polish Polar Research* 27: 309–326.

GRABIEC M., PUCZKO D., BUDZIK T. and GAJEK G. 2011. Snow distribution patterns on Svalbard glaciers derived from radio-echo soundings. *Polish Polar Research* 32: 393–421.

GRABIEC M., JANIA J., PUCZKO D., KOLONDRA L. and BUDZIK T. 2012. Surface and bed morphology of Hansbreen, a tidewater glacier in Spitsbergen. *Polish Polar Research* 33: 111–138.

HAGEN J.O., MELVOLD K., PINGLOT F. and DOWDESWELL J.A. 2003. On the net mass balance of the glaciers and ice caps in Svalbard, Norwegian Arctic. *Arctic, Antarctic, and Alpine Research* 35: 264–270.

HARTMAN M.D., BARON J.S., LAMMERS R.B., CLINE D.W., BAND L.E., LISTON G.E. and TAGUE C. 1999. Simulations of snow distribution and hydrology in a mountain basin. *Water Resources Research* 35: 1587–1603.

HOCK R. 2003. Temperature index melt modelling in mountain areas. *Journal of Hydrology* 282: 104–115.

IGNATIUK D., PIECHOTA A.M., CIEPŁY M. and LUKS B. 2014. Changes of altitudinal zones of Werenskioldbreen and Hansbreen in period 1990 – 2008, Svalbard. *AIP Conference Proceedings* 1618: 275.

IRVINE-FYNN T.D.L., HODSON A.J., MOORMAN B.J., VATNE G. and HUBBARD A.L. 2011. Polythermal glacier hydrology: A review. *Reviews of Geophysics* 49: RG4002.

ISMAIL M.F., REHMAN H., BOGACKI W. and MUHAMMAD N. 2015. Degree Day Factor models for forecasting the snowmelt runoff for Naran watershed. *Science International* 27: 1951–1960.

JAEDICKE C. and GAUER P. 2005. The influence of drifting snow on the location of glaciers on western Spitsbergen, Svalbard. *Annals of Glaciology* 42: 237–242.

JANIA J. and HAGEN J.O. 1996. *Mass balance of Arctic Glaciers*. IASC, University of Silesia, Sosnowiec-Oslo: 62 pp.

JANIA J. and KACZMARSKA M. 1997. Hans Glacier – a tidewater glacier in southern Spitsbergen: summary of some results. *In*: Van der Veen (ed.) *Calving Glaciers: Report of a Workshop*, BPRC Report No 15, Byrd Polar Research Center, The Ohio State University, Columbus, Ohio: 95–104.

JANSSON P., HOCK R. and SCHNEIDER T. 2003. The concept of glacier storage: a review. *Journal of Hydrology* 282: 116–129.

KĘPSKI D., GÓRSKI Z., BENEDYK M. and SZUMNY M. 2013. Meteorological Bulletins, Spitsbergen – Hornsund. *Polish Polar Station Institute of Geophysics Polish Academy of Sciences*.https://hornsund.igf.edu.pl/Biuletyny/BIULETYN_36

KOENIGK T., BERG P. and DÖSCHER R. 2015. Arctic climate change in an ensemble of regional CORDEX simulations. *Polar Research* 34: 24603.

KOHAVI R. 1995. A study of cross-validation and bootstrap for accuracy estimation and model selection. *Proceedings of the 14th International Joint Conference on Artificial Intelligence* 2: 1137–1145.

KORONA J., BERTHIER E., BERNARD M., RÉMY F. and THOUVENOT E. 2009. SPIRIT. SPOT 5 stereoscopic survey of Polar Ice: Reference Images and Topographies during the fourth International Polar Year (2007–2009), ISPRS. *ISPRS Journal of Photogrammetry and Remote Sensing* 64: 204–212.

KRASTING J.P., BROCCOLI A.J., DIXON K.W. and LANZANTE J.R. 2013. Future changes in Northern Hemisphere snowfall. *Journal of Climate* 26: 7813–7828.

LASKA M., LUKS B. and BUDZIK T. 2016. The influence of the snowpack internal structure on snow metamorphism and melting intensity (Hansbreen, Svalbard). *Polish Polar Research* 37: 193–218.

LASKA M., GRABIEC M., IGNATIUK D. and BUDZIK T. 2017a. Snow deposition patterns on southern Spitsbergen glaciers, Svalbard, in relation to recent meteorological conditions and local topography. *Geografiska Annaler*: Series A, Physical Geography 99: 262–287.

LASKA M., BARZYCKA B. and LUKS B. 2017b. Melting characteristics of snow cover on tidewater glaciers of Hornsund fjord, Svalbard. *Water* 9: 804.

ŁASZYCA E., PERCHALUK J., KĘPSKI D., GÓRSKI Z. and WAWRZYNIAK T. 2014. Meteorological Bulletins, Spitsbergen – Hornsund. *Polish Polar Station Institute of Geophysics Polish Academy of Sciences*. https://hornsund.igf.edu.pl/Biuletyny/BIULETYN_37

ŁUPIKASZA E. 2013. Atmospheric precipitation. *In*: Marsz A.A. and Styszyńska A. (eds); *Climate and Climate Change at Hornsund, Svalbard*. Gdynia Maritime University, Gdynia: 199–211.

ŁUPIKASZA E.B., IGNATIUK D., GRABIEC M., CIELECKA-NOWAK K., LASKA M., JANIA J., LUKS B., USZCZYK A. and BUDZIK T. 2019. The Role of Winter Rain in the Glacial System on Svalbard. *Water* 11: 334.

MARSH P. 1999. Snowcover formation and melt: recent advances and future prospects. *Hydrological Processes*, 13: 2117–2134.

MARSZ A.A. 2013. Air temperature. *In*: Marsz A.A. and Styszyńska A. (eds) *Climate and Climate Change at Hornsund, Svalbard*. Gdynia Maritime University, Gdynia: 145–187.

MIGAŁA K., PEREYMA J. and SOBIK M. 1988. Snow accumulation in southern Spitsbergen. *Prace Naukowe Uniwersytetu Śląskiego* 910: 48–63.

MIGAŁA K., PIWOWAR B.A. and PUCZKO D. 2006. A meteorological study of the ablation process on Hans Glacier, SW Spitsbergen. *Polish Polar Research* 27: 243–258.

MILLER G.H., ALLEY R.B., BRIGHAM-GRETTE J., FITZPATRICK J.J., POLYAK L., SERREZE M.C. and WHITE J.W. 2010. Arctic amplification: can the past constrain the future? *Quaternary Science Reviews* 29: 1779–1790.

MORTENSEN J., BENDTSEN J., MOTYKA R.J., LENNERT K., TRUFFER M., FAHNESTOCK M. and RYSGAARD S. 2013. On the seasonal freshwater stratification in the proximity of fast-flowing tidewater outlet glaciers in a sub-Arctic sill fjord. *Journal of Geophysica Research* 118: 1382–1395.

MÖLLER M., OBLEITNER F., REIJMER C.H., POHJOLA V.A., GŁOWACKI P. and KOHLER J. 2016. Adjustment of regional climate model output for modeling the climatic mass balance of all glaciers on Svalbard. *Journal of Geophysical Research: Atmospheres* 121: 5411–5429.

NORDLI Ø., PRZYBYLAK R., OGILVIE A.E. and ISAKSEN K. 2014. Long-term temperature trends and variability on Spitsbergen: the extended Svalbard Airport temperature series, 1898–2012. *Polar Research* 33: 21349.

NUTH C., MOHOLDT G., KOHLER J., HAGEN J.O. and KÄÄB A. 2010. Svalbard glacier elevation changes and contribution to sea level rise. *Journal of Geophysical Research* 115: F01008.

NUTH C., KOHLER J., KÖNIG M., DESCHWANDEN A.V., HAGEN J.O.M., KÄÄB A. and PETTERSSON R. 2013. Decadal changes from a multi-temporal glacier inventory of Svalbard. *The Cryosphere* 7: 1603–1621.

OERLEMANS J., JANIA J. and KOLONDRA L. 2011. Application of a minimal glacier model to Hansbreen, Svalbard. *The Cryosphere* 5: 1–11.

OHMURA A. 2001. Physical basis for the temperature based melt index method. *Journal of Applied Meteorology* 40: 753–761.

PARRY V., NIENOW P., MAIR D., SCOTT J., HUBBARD B., STEFFEN K. and WINGHAM D. 2007. Investigations of meltwater refreezing and density variations in the snowpack and firn within the percolation zone of the Greenland ice sheet. *Annals of Glaciology* 46: 61–67.

PFEFFER W.T. and HUMPHREY N.F. 1998. Formation of ice layers by infiltration and refreezing of meltwater. *Annals of Glaciology* 26: 83–91.

RÄISÄNEN J. 2008. Warmer climate: Less or more snow? *Climate Dynamics* 30: 307–319.

SHERIFF R.E. 1977. Limitations on resolution of seismic reflections and geologic detail derivable from them. *In*: Payton C.E. (ed) *Seismic Stratigraphy-Applications to Hydrocarbon Exploration*. *AAPG Mem*oir 16: 3–14.

STRANEO F., CURRY R.G., SUTHERLAND D.A., HAMILTON G.S., CENEDESE C., VÅGE K. and STEARNS A. 2011. Impact of fjord dynamics and glacial runoff on the circulation near Helheim Glacier. *Nature Geoscience* 4: 322–327.

STURM M., TARAS B., LISTON G.E., DERKSEN C., JONAS T. and LEA J. 2010. Estimating snow water equivalent using snow depth data and climate classes. *Journal of Hydrometeorology* 11: 1380–1394.

STYSZYŃSKA A. 2013. The winds. *In*: Marsz A.A. and Styszyńska A. (eds) *Climate and Climate Change at Hornsund, Svalbard*. Gdynia Maritime University, Gdynia: 81–99.

SZAFRANIEC J. 2002. Influence of positive degree-days and sunshine duration on the surface ablation of Hansbreen, Spitsbergen glacier. *Polish Polar Research* 23: 227–240.

VAN DEN BROEKE M., BUS C., ETTEMA J. and SMEETS P. 2010. Temperature thresholds for degree--day modelling of Greenland ice sheet melt rates. *Geophysical Research Letters* 37: L18501.

VAN PELT W.J.J., POHJOLA V.A., PETTERSSON R., EHWALD L.E., REIJMER C.H., BOOT W. and JAKOBS C.L. 2018. Dynamic response of a High Arctic glacier to melt and runoff variations. *Geophysical Research Letters* 45: 4917–4926.

VIELI A., JANIA J. and KOLONDRA L. 2002. The retreat of a tidewater glacier: observations and model calculations on Hansbreen, Spitsbergen. *Journal of Glaciology* 48: 592–600.

VIELI A., JANIA J., BLATTER H. and FUNK M. 2004. Short-term velocity variations on Hansbreen, a tidewater glacier in Spitsbergen. *Journal of Glaciology* 50: 389–398.

WGMS. 2012. Fluctuations of Glaciers 2005–2010, Volume X. Zemp M., Frey H., Gärtner-Roer I., Nussbaumer S.U., Hoelzle M., Paul F., and Haeberli W. (eds) ICSU(WDS)/ IUGG(IACS)/UNEP/ UNESCO/WMO, World Glacier Monitoring Service, Zurich, Switzerland: 336 pp.

WGMS. 2015. Global Glacier Change Bulletin No. 1 (2012–2013). Zemp M., Gärtner-Roer I., Nussbaumer S.U., Hüsler F., Machguth H., Mölg N., Paul F., and Hoelzle M. (eds) ICSU(WDS)/ IUGG(IACS)/UNEP/UNESCO/WMO, World Glacier Monitoring Service, Zurich, Switzerland: 230 pp.

WILLIS I.C. 1995. Intra-annual variations of glacier motion: a review. *Progress in Physical Geography* 19: 61–106.

WINTHER J.-G., BRULAND O., SAND K., GERLAND S., MARECHAL D., IVANOV B., GŁOWACKI P. and KÖNIG M. 2003. Snow research in Svalbard. *Polar Research* 22: 125–144.

Received 1 April 2019
Accepted 9 October 2019